

Supporting Information

A ductile and strong-affinity network binder coupling inorganic oligomers and biopolymers for high-loading lithium-sulfur batteries

Mingxiu Hou^{a, b}, Jie Liu^{a, c, *}, Fengli Yu^{a, b}, Lei Wang^{a, b, *}

^a *State Key Laboratory Base of Eco-chemical Engineering, International Science and Technology Cooperation Base of Eco-chemical Engineering and Green Manufacturing, Qingdao University of Science and Technology, Qingdao 266042, China*

E-mail: jie.liu@qust.edu.cn (J. Liu), inorchemwl@126.com (L. Wang)

^b *College of Chemistry and Molecular Engineering, Qingdao University of Science and Technology, Qingdao 266042, China*

^c *College of Chemical Engineering, Qingdao University of Science and Technology, Qingdao 266042, China*

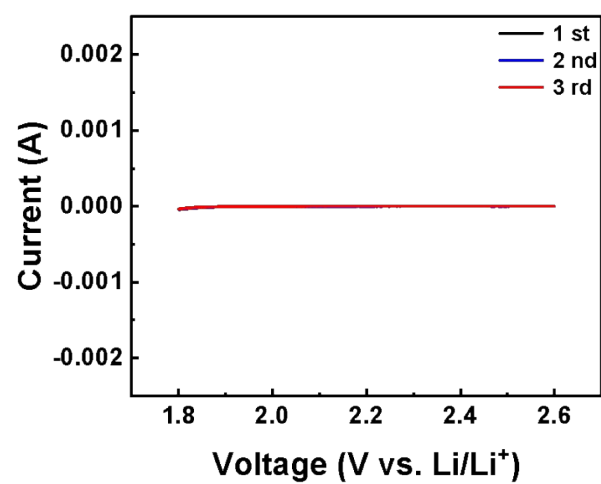


Fig. S1. Cyclic voltammetry (CV) curves of the KB@TSG-PTP electrode at a scan rate of 0.1 mV s^{-1} .

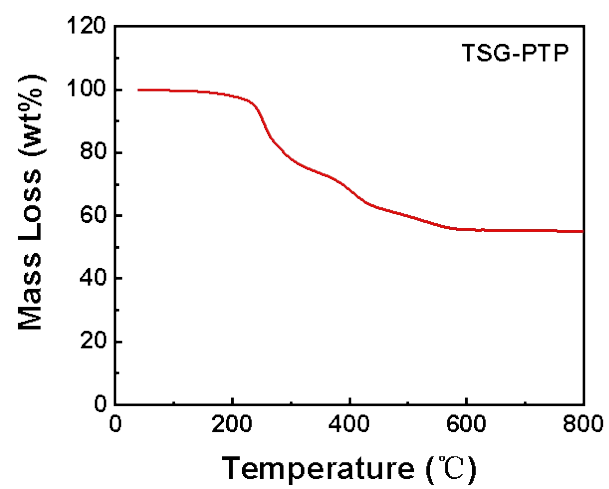


Fig. S2. TGA curve of TSG-PTP under the air atmosphere with the heating rate of 10 °C min⁻¹.

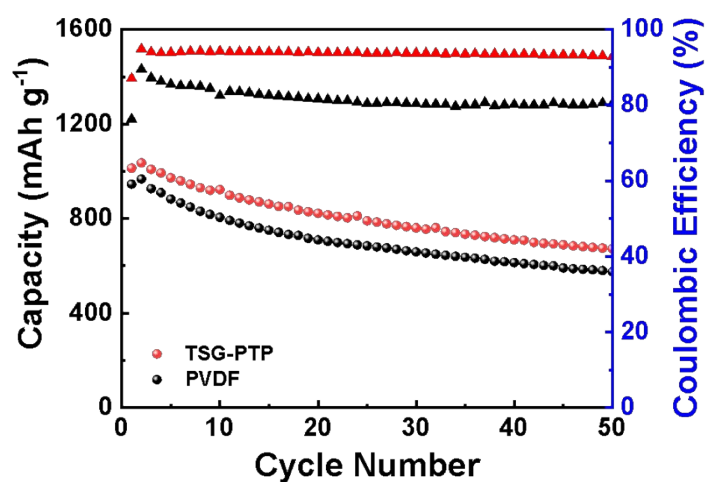


Fig. S3. Cycling performance of Li-S batteries using different binders at 0.2 C (the first cycle is at 0.1 C). The sulfur cathodes consist of 80 wt% S/super P composite, 10 wt% KB, and 10 wt% binder. The electrolyte is 1M LiTFSI in DOL : DME (1:1 Vol%) without LiNO₃ additive.

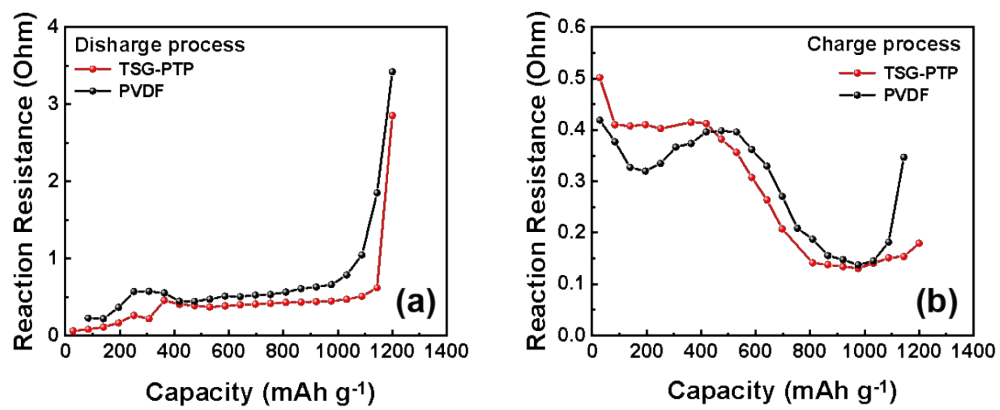


Fig. S4. Comparison of reaction resistances of sulfur electrodes with different binders

(a) during discharge process and (b) during charge process.

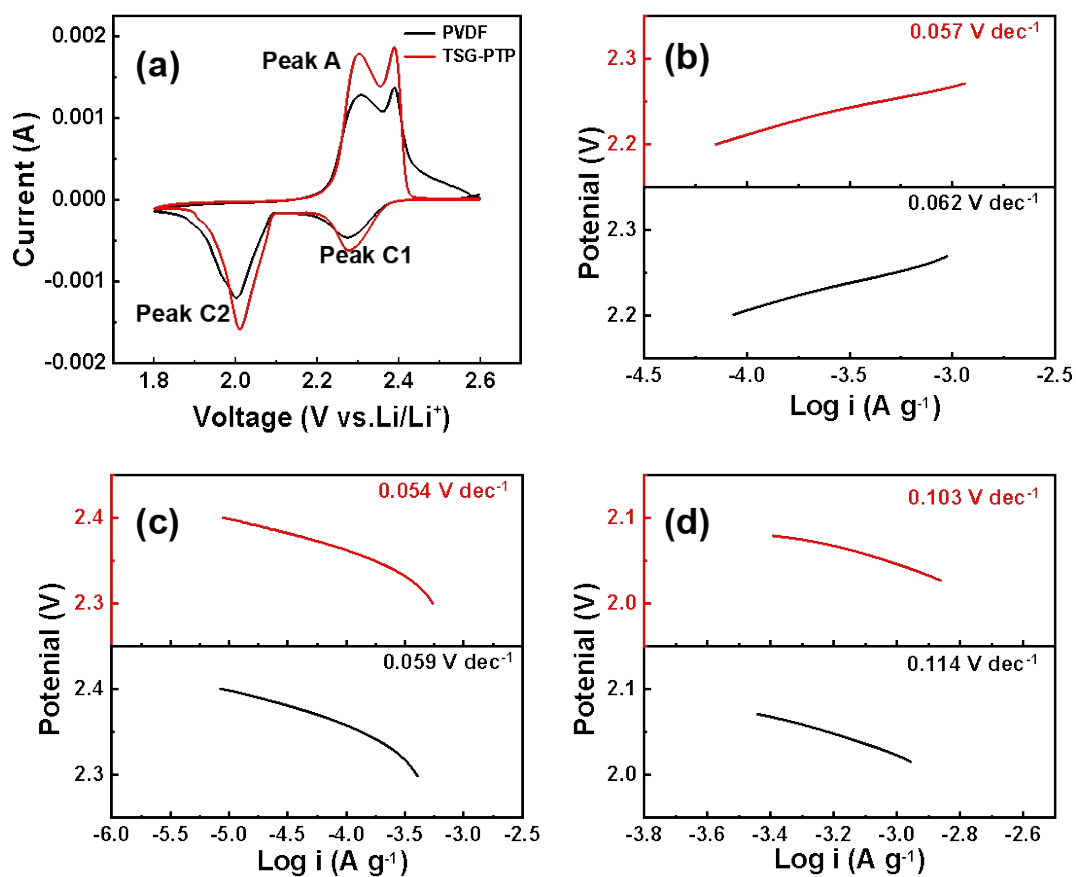


Fig. S5. (a) CV curves of the sulfur electrodes with different binders at a scan rate of 0.1 mV s^{-1} . Tafel plots of (b) peak A, (c) peak C1, and (d) peak C2 in (a).

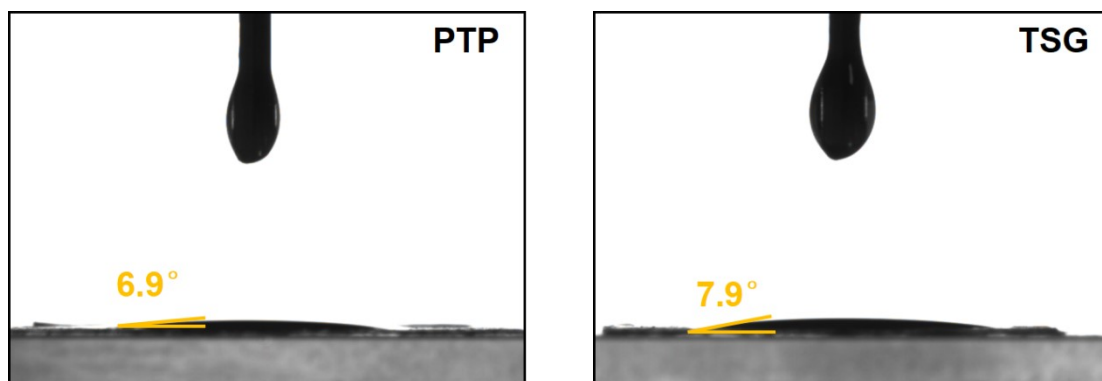


Fig. S6. Contact angle of the electrolyte towards S@PTP electrode and S@TSG electrode.

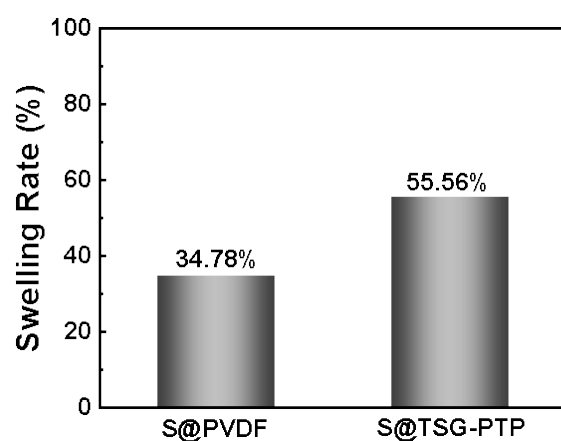


Fig. S7. The swelling rate of S@PVDF and S@TSG-PTP electrodes after immersion in electrolyte for 24 h. The swelling rate is defined as $(W_{24}-W_0)/W_0*100\%$, where W_{24} is the weight of electrode coating after immersion in electrolyte for 24 h, W_0 is the weight of electrode coating before immersion in electrolyte.

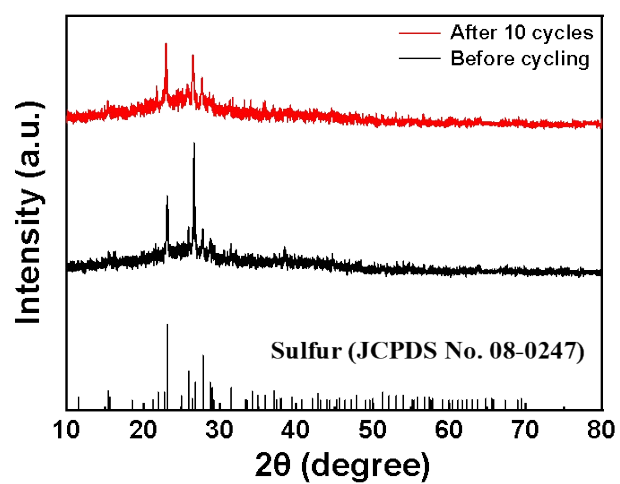


Fig. S8. XRD patterns of S@TSG-PTP electrode before cycling and after 10 cycles.

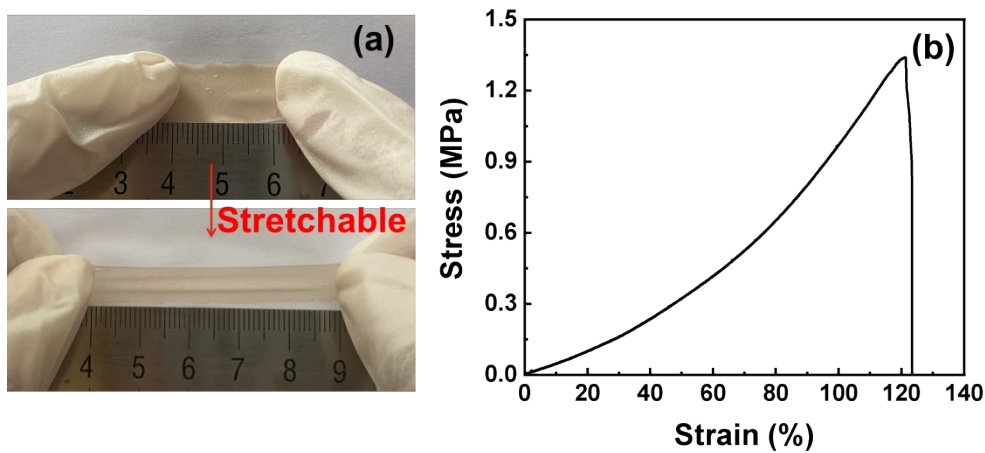


Fig. S9. (a) Optical photographs of the TSP-PTP film showing its stretchability; (b) stress-strain curve of TSP-PTP film.

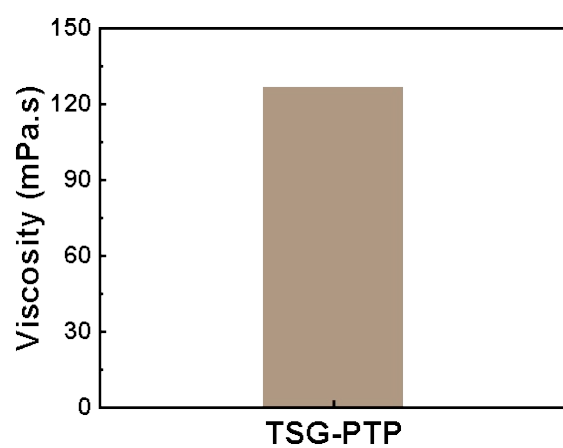


Fig. S10. Viscosity of 2 wt% TSG-PTP aqueous solution obtained by rotor 3 on a viscosity analyzer (Techcomp SNP-1).

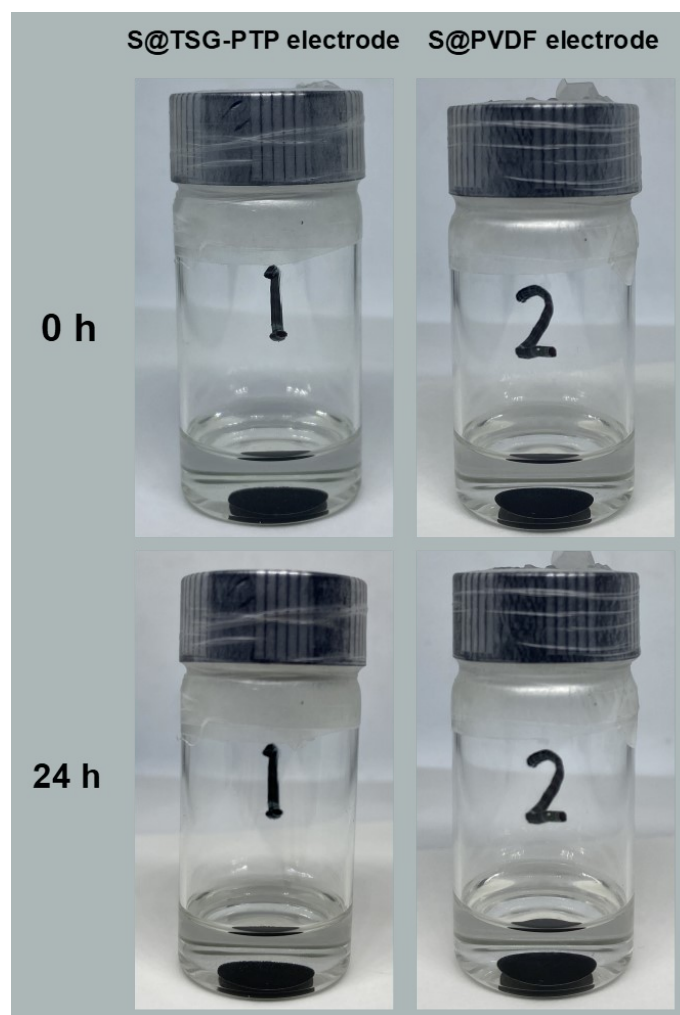


Fig. S11. Photographs of the S@TSG-PTP electrode and S@PVDF electrode soaked in the electrolyte after 0 h and after 24 h.

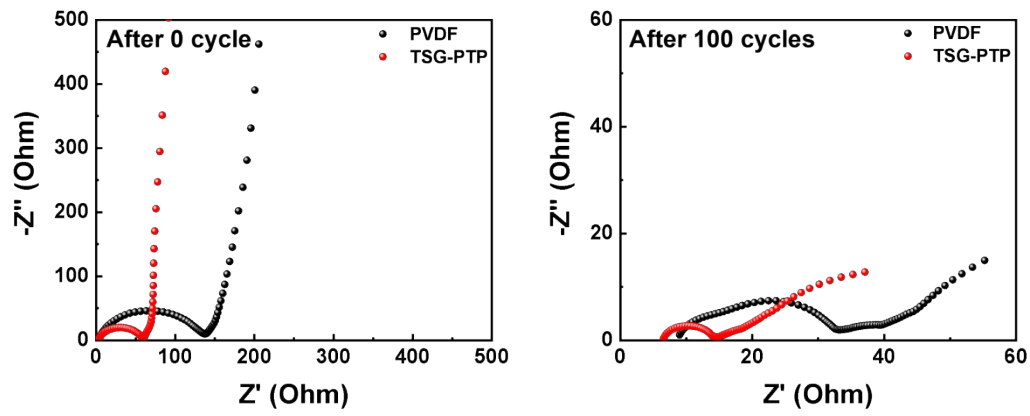


Fig. S12. The Nyquist plots of Li-S batteries with PVDF and TSG-PTP binders after 0 cycle and 100 cycles at 0.5 C.

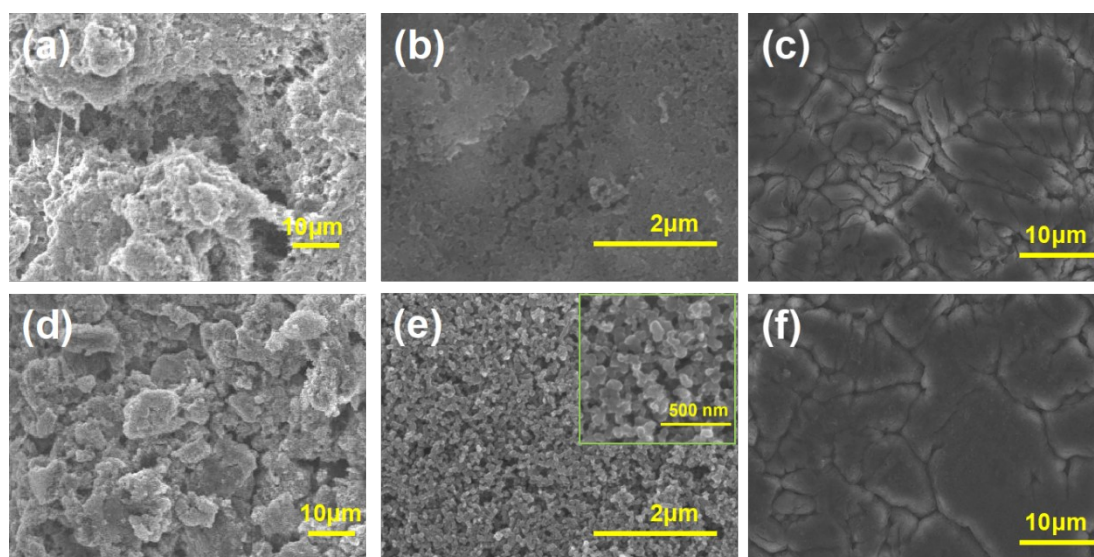


Fig. S13. SEM images of S@PVDF electrode (a) before cycling and (d) after 50 cycles, S@TSG-PTP electrode (b) before cycling and (e) after 50 cycles; SEM images of the lithium anodes after 50 cycles with (c) S@PVDF electrode, (f) S@TSG-PTP electrode.